A viroporin-like 2B protein of duck hepatitis A virus 1 that induces incomplete autophagy in DEF cells

Zezheng Liu,[*,†,‡] Qian Ye,[*,†,‡,1] Anchun Cheng,[*,†,‡,1] Xumin Ou,[*,†,‡] Sai Mao,[*,†,‡] Di Sun,[*,†,‡] Shaqiu Zhang,[*,†,‡] Xinxin Zhao,[*,†,‡] Qiao Yang,[*,†,‡] Ying Wu,[*,†,‡] Juan Huang,[*,†,‡] Qun Gao,[*,†,‡] Bin Tian,[*,‡] and Mingshu Wang[*,†,‡,2]

[*]*Institute of Preventive Veterinary Medicine, Sichuan Agricultural University, Wenjiang, Chengdu City, Sichuan, 611130, P.R. China;* [†]*Key Laboratory of Animal Disease and Human Health of Sichuan Province, Sichuan Agricultural University, Wenjiang, Chengdu City, Sichuan, 611130, P.R. China; and* [‡]*Avian Disease Research Center, College of Veterinary Medicine, Sichuan Agricultural University, Wenjiang, Chengdu City, Sichuan, 611130, P.R. China*

ABSTRACT Duck hepatitis A virus 1 (**DHAV-1**) can cause high morbidity and fatal acute infectious hepatitis in ducklings, which seriously endangers animal husbandry. Viroporin is a small molecular weight hydrophobic transmembrane protein encoded by the virus, that has been suggested to induce autophagy in host cells by increasing the membrane permeability through disturbing the ion balance. In this study, we aimed to investigate whether the DHAV-1 2B protein can induce autophagy in DEF cells with a viroporin-like function. Bioinformatics analysis has indicated that the 2B protein is characterized by a viroporin domain, which is consistent with the type IA viroporin transmembrane protein. We experimentally confirmed that the 2B protein disturbed the Ca2+ balance of infected cells by elevating the intracellular Ca2+ concentration. Eukaryotic expression of the 2B protein upregulates the expression of microtubule-associated protein 1 light chain 3 II (**LC3-II**) and the number of autophagosomes in the cell. Interestingly, the Western Blot (**WB**) results showed that 2B protein expression induced less protein degradation of the autophagic substrate sequestosome 1 **(SQSTM1/p62)** than the positive control, while microscopy observations showed that the autophagosomes did not colocalize with the lysosomes. In summary, 2B protein expression induced autophagy in host cells, but the autophagic flow was incomplete. The results of this experiment are expected to provide reference scientific data for elucidating the infective and pathogenic mechanism of DHAV-1.

Key words: duck hepatitis A virus 1, 2B protein, viroporin, autophagy

2021 Poultry Science 100:101331
https://doi.org/10.1016/j.psj.2021.101331

INTRODUCTION

Duck hepatitis A virus (**DHAV**) infection can cause high morbidity and highly lethal acute infectious hepatitis with clinical symptoms such as liver enlargement and neurological disorders, and seriously endangers animal husbandry (Ou et al., 2017b; Ou et al., 2017c; Wen et al., 2018). Most studies on DHAV mainly focus on its etiology, pathogenesis, epidemiology, and diagnosis (Yang et al., 2008; Cheng et al., 2009; Wen et al., 2014; Shen et al., 2015; Hu et al., 2016; Mao et al., 2016; Mao et al., 2017; Ou et al., 2017a; Xie et al., 2018b; Xie et al., 2018a; Zhou et al., 2019). A variety of excellent live attenuated vaccines have been developed for this disease (Haijun et al., 2007; Yang et al., 2008; Song et al., 2014; Ou et al., 2018), which has led to it being well controlled in many areas. DHAV can be divided into 3 genotypes, namely DHAV-1, DHAV-2, and DHAV-3.

DHAV-1, a member of the genus *Avihepadnavirus* within the family *Picornaviridae*, is a nonenveloped, positive single-stranded RNA virus. The complete genome structure of DHAV-1 is VPG + 5′-untranslated region (**UTR**)-open reading fame (**ORF**)-3′-UTR + Poly (A), with a length of approximately 7.7 kilobase **(kb)** pairs (Kim et al., 2006; Ding and Zhang, 2007; Tseng et al., 2007). The viral genome encodes a polyprotein precursor, which is divided into the regions P1, P2 and P3, and is processed by the virus-encoded 2A, 3C and 3CD proteases. Processing of the

Received May 10, 2020.
Accepted June 4, 2021.

[1]These authors contributed equally to this work as first authors.

[2]Corresponding author: mshwang@163.com

P1 region produces the structural capsid proteins VP0, VP3, and VP1, whereas the P2 and P3 regions are processed into the nonstructural proteins $2A_{1\text{-}3}$, 2B, 2C, 3A, 3B (VPg), 3C and 3D as well as cleavage intermediates (2BC, 3AB, and 3CD); protein 2B is a nonstructural protein with a total of 357 bases encoding 119 amino acids (Wen et al., 2015; Mao et al., 2016; Yang et al., 2017; Xiaoyao et al., 2018).

Viroporin is a small molecular weight hydrophobic transmembrane protein encoded by virus and possesses 1 to 3 hydrophobic transmembrane domains. According to the number of hydrophobic transmembrane domains and the transmembrane mode, the viroporin family can be roughly divided into the types IA, IB and IIA, IIB (Nieva et al., 2012; Luis Nieva and Carrasco, 2015). These hydrophobic transmembrane regions can interact with the phospholipid bilayer in the form of multimers to alter the permeability of the host cell membrane, which in turn disrupts the physiological functions of the host cell to ensure that the virus can complete its full life cycle (Gonzalez and Carrasco, 2003; Nieva et al., 2012; Giorda and Hebert, 2013; Hyser and Estes, 2015). The viroporin family has the functions of promoting virus entry, proliferation and release (McLean et al., 2011b), disrupting the ion balance in the body (Crawford et al., 2012b), regulating host cell apoptosis (Bagchi et al., 2010) and promoting host cell autophagy (Gannage et al., 2009b).

Autophagy is one of the main pathways involved in protein quality control in eukaryotic cells and occurs in cells at a low-basic level, such as those undergoing starvation or viral infection, and causes the degradation of misfolded proteins and damaged organelles to produce amino acids and adenosine triphosphate (**ATP**), thereby maintaining cell homeostasis and normal physiological functions (Levine and Kroemer, 2008; Levine et al., 2011; Shan et al., 2017; Wu et al., 2019). Three types of autophagy have been identified in mammalian cells: macroautophagy, microautophagy and chaperone-mediated autophagy (Sun et al., 2019a). Macroautophagy (hereafter referred to as autophagy) is an evolutionarily conserved process, in which the cytoplasmic components are sequestered within cytosolic double-membrane vesicles and then delivered to lysosomes for degradation. During autophagy, crescent-shaped vesicles from the endoplasmic reticulum (**ER**)/ Golgi apparatus (**Golgi**) phagocytose mitochondria and other organelles to form phagocytic vacuoles (Xie and Klionsky, 2007; Landajuela et al., 2016). The phagocytic bubble gradually extends and closes into a complete bilayer membrane structure. Subsequently, autophagosomes can fuse with endosomes to form autophagic endosomes which can then fuse with lysosomes to form autophagosomes. In addition, autophagosomes can directly fuse with lysosomes to form autophagosomes (Lamb et al., 2013; Nakatogawa, 2013). Finally, the contents, such as mitochondria, contained within the autophagosomes are degraded (Ni et al., 2011).

Many picornavirus 2B proteins, such as coxsackievirus B (**CBV**), foot-and-mouth disease virus (**FMDV**), and hepatitis A virus (**HAV**) 2B, have been shown to have viroporin properties. In addition, these proteins can cause the spot-like aggregation of microtubule-associated protein 1 light chain 3 (**LC3**) in cells after transfection, and CBV and FMDV 2B proteins also show colocalization with autophagosomes, which indicates that expression of 2B protein can induce host cells undergo autophagy (Monika et al., 1998; Guo et al., 2015; Heng et al., 2016). At present, there are fewer studies on DHAV-1 2B protein compared with other picornaviruses, and the current research focus is mainly on CBV and FMDV. The molecular and functional characteristics of the DHAV-1 2B protein remain to be studied, such as whether the DHAV-1 2B protein has viroporin properties similar to other picornavirus 2B proteins, what the effects of the 2B protein are on the ion gradient in host cells, and whether the 2B protein can induce host cells to undergo autophagy and the mechanisms involved. In this study, the molecular characteristics and functional analysis of the DHAV-1 2B protein were used to investigate the viroporin characteristics of the 2B protein and its effect on host cell autophagy.

MATERIALS AND METHODS

Cell, Plasmids, and Virus

The DHAV-1 H strain (GenBank accession number: JQ301467.1), the eukaryotic expression vector pCAGGS, GFP-LC3 and mRFP-GFP-LC3 plasmids were all preserved and provided by the Poultry Disease Control and Research Center of Sichuan Agricultural University. Duck embryo fibroblasts (**DEF**) were prepared from duck embryos aged 9 to 11 d purchased from Ya'an, Sichuan Province and cultured in MEM (Thermo Scientific, Wilmington, NC) supplemented with 10% calf serum (Thermo Scientific, Wilmington, NC) at 37°C in the presence of 5% CO_2 as described previously (Lai et al., 2019; Xie et al., 2019).

Reagents and Antibodies

Fluo-3 AM and Lyso-Tracker Red were purchased from Beyotime (Shanghai, China). Rapamycin was purchased from Sigma-Aldrich (St. Louis, MO). Rabbit anti-LC3 antibody and rabbit anti-SQSTM1 / p62 antibody were purchased from Cell Signaling Technology (Danvers, MA). Rabbit anti-β-actin antibody, rabbit anti-FLAG polyclonal antibody, HRP-conjugated anti-rabbit IgG were purchased from Beyotime. Alexa Fluor 594- conjugated anti-rabbit IgG was purchased from Thermo Scientific. Rabbit anti-HA monoclonal antibody was purchased from Proteintech Group (Rosemont, IL).

Plasmid Construction

The procedure was performed as described previously and modification slightly (Sun et al., 2019b). Briefly, to construct eukaryotic recombinant plasmids pCAGGS-

Table 1. Primer design of eukaryotic recombinant plasmid.

Recombinant plasmid	Primer design (Sequences 5'to 3')	Restriction sites
pCAGGS-2B-HA	F: CATCATTTTGGCAAAGAATTCGCCACCATGGCCTCATTTCCAGGTAAAGATGC	EcoR I
	R: TTGGCAGAGGGAAAAAGATCTTCAAGCGTAGTCTGGGACGTCGTATGGGT ATTGATCCTCTAACATGTCATTG	Hind III
pCAGGS-Flag-2B	F: CATCATTTTGGCAAAGAATTCGCCACCATGGATTACAAGGATGACGACGAT AAGTCATTTCCAGGTAAAGATGC	EcoR I
	R: TTGGCAGAGGGAAAAAGATCTTCATTGATCCTCTAACATGTCATTG	Hind III

Note: F (Forward primer); R (Reverse primer).

2B-HA and pCAGGS-FLAG-2B, DHAV-1 genomic RNA was extracted from the culture supernatants of DEF cells that were infected with DHAV-1. Single stranded cDNA was then synthesized from the purified virus RNA by reverse transcription (TaKaRa, Dalian, China). The 2B-HA and Flag-2B genes were amplified from the cDNA by Polymerase chain reaction (**PCR**) using primers listed in (Table 1). PCR products were cloned into the pCAGGS vector to construct the recombinant plasmids pCAGGS-2B-HA and pCAGGS-FLAG-2B respectively. The recombinant plasmid was confirmed by plasmid sequencing and Western Blot.

Transfection

DEF cells were prepared and cultured in a 6-well culture dish. When the cell density reached 90%, the manufacturer's instructions of the TransIntro EL Transfection Reagent (TransGen Biotech, Beijing, China) were used. The plasmid was diluted in MEM and then the transfection reagent was added. After mixing, the plasmid transfection reagent complex was added to the cell culture dish.

Western Blot

The procedure was performed as described previously and modification slightly (Zhang et al., 2017). Briefly, the cells were lysed with RIPA (Beyotime Biotechnology) containing protease inhibitor and 1% Phenylmethylsulfonylfluoride (**PMSF**, Beyotime Biotechnology), and the supernatant was separated by 12% SDS-PAGE electrophoresis. After electrophoresis, the target protein was transferred from PAGE gel to a nitrocellulose membrane (PVDF, Millipore, MO). Subsequently, the membrane was blocked and incubated with rabbit anti-HA (Proteintech Group, Rosemont, IL), rabbit anti-FLAG (Beyotime Biotechnology), rabbit anti-LC3 (Cell Signaling Technology, Danvers, MA), rabbit anti-SQSTM1/p62 (Cell Signaling Technology, Danvers, MA) or rabbit anti-β-actin antibodies (Beyotime Biotechnology), followed by incubation with HRP-conjugated anti-rabbit IgG (Beyotime Biotechnology). Finally, the protein signal was displayed by an enhanced chemiluminescence (**ECL**) Western blotting analysis system.

Immunofluorescence Assay

The procedure was performed as described previously and modification slightly (Sun et al., 2017). Briefly, after collecting the slides, the cells were fixed with 4% paraformaldehyde at 4°C overnight and then permeabilized at 4°C for 30 min. Subsequently, the slides were blocked with 5% BSA (Bio-Rad, Hercules, CA) for 1 h at 37°C, incubated with the primary antibody at 4°C overnight, followed by incubation with the fluorescently labeled secondary antibody at 37°C for 1 h and staining with 4′,6-diamidino-2-phenylindole (**DAPI**). The image was taken and observed by the Olympus BX43 after glycerol fixation.

Prediction of Viroporin Motifs in 2B Protein

The gene sequence of the 2B protein of the DHAV-1 H strain (GenBank accession number: JQ301467.1) given in the NCBI was introduced into the Biosequence Analysis Center (**CBS**) website of the Technical University of Denmark (website http://genome.cbs.dtu.dk/services/TMHMM/) for transmembrane prediction. Secondary structure was performed using PSIPred prediction analysis suite (website http://bioinf.cs.ucl.ac.uk/introduction/) (Buchan and Jones, 2019). Kyte and Doolittle Hydropathy and Amphipathic moment plots were generated by using the Hydropathy Analysis program at the Transporter Classification Database (website http://www.tcdb.org) (Saier et al., 2006).

Prediction Of 2B Protein Transmembrane Mode in DEF Cells

TransIntro EL transfection reagent (TransGen Biotech, Beijing, China) was used to transfect plasmids pCAGGS-2B-HA and pCAGGS-FLAG-2B into DEF cells respectively, and the slides were collected at 48-h post-transfection. After the cells were fixed with paraformaldehyde, one group was permeabilized with 0.25% Triton-100; the other group was permeabilized with digitalis saponin (0.01 mg / mL). Then the cells were blocked with 5% BSA in PBS and specific antibodies were incubated. The results were observed with a fluorescence microscope after glycerol fixation.

Detection of Intracellular Ca2+ Concentrations

Transfect pCAGGS-2B-HA into DEF cells, and set the pCAGGS transfection group as a negative control. Three biological replicates were set per group. At 48 h post-transfection, the cells were treated with Fluo-3 AM

(Beyotime Biotechnology) with reference to the instructions. Fluorescence detection was performed using a multifunction microplate reader (Thermo Scientific) at 488 nm excitation and 525 nm emission wavelength.

mRFP-GFP-LC3 Dual Fluorescence Indicator System

After transfection of 2.0 μg of the mRFP-GFPLC3 plasmid into DEF cells, one group was cotransfected with 2.0 μg of pCAGGS-2B-HA while the other group was left untreated as a negative control. The remaining 2 groups were starved or treated with rapamycin 4 h before harvest as a positive control. Cell slides were collected at 48-h post-transfection, and DAPI was stained after fixation and permeation. The results were observed with a fluorescence microscope after glycerol fixation.

Lysosomal Staining

Using Lyso-Tracker Red to stain lysosomes to detect the colocalization of autophagosomes and lysosomes. After transfection of 2.0 μg of the GFP-LC3 plasmid into DEF cells, one group was cotransfected with 2.0 μg of pCAGGS-2B-HA while the other group was left untreated as a negative control. The remaining 2 groups were starved or treated with rapamycin 4 h before harvest as a positive control. Cell slides were collected at 48-h post-transfection, washed 3 times with 1 × PBS, 200 μL 0.05 μM Lyso-Tracker Red was added and incubated at 37°C for 40 min. Subsequently, the slides were fixed with 4% paraformaldehyde overnight at 4°C, permeabilized with 0.25% Triton X-100 (Beyotime) at 4°C for 30 min and staining with DAPI. Images was taken and observed by the Olympus BX43 after glycerol fixation.

Statistical Analysis

Statistics and plotting were performed by GraphPad Prism (version 8.02). Data are presented as means ± standard deviations (n = 3). Significance difference was determined by Student's t test. P values less than 0.05 were considered as significance.

RESULTS

Prediction of Viroporin Motifs in 2B Protein

The transmembrane domain (**TMD**) prediction results show that there is only one transmembrane region in the 2B protein (Figure 1A), which is located between the 41st amino acid and the 63 rd amino acid. Next, we constructed a Kyte-Doolittle plot to detect the hydrophobic regions of 2B and an amphipathicity plot to identify potential amphipathic domains (Figure 1B). We found that the predicted TMD is extremely hydrophobic and amphiphilic, and secondary structure

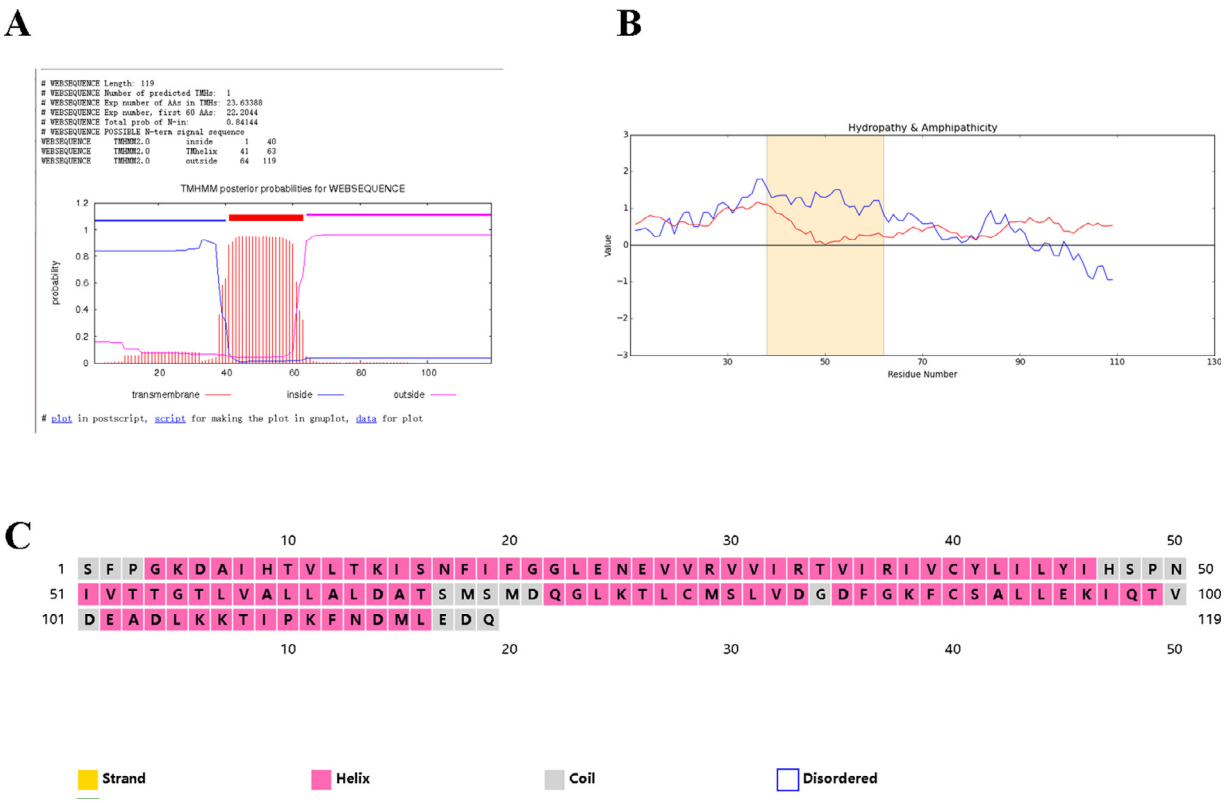

Figure 1. Prediction of viroporin motifs in 2B Protein. (A) Transmembrane prediction. Blue baseline represents the fragment toward the intramembrane, pink baseline represents the fragment toward the outside of the membrane, and red baseline represents the transmembrane region. (B) Kyte-Doolittle hydropathy plots. Blue lines denote hydropathy and red lines denote amphipathicity. (C) PSIPred secondary structure algorithms prediction.

analysis suggested that the 2B protein was predominantly composed of α-helices. Studies have shown that viroporin family proteins have some common characteristics, which can be considered the basis for viroporin identification. First, viroporins are small integral membrane proteins, typically approximately 100 aa in length. Second, viroporins are generally hydrophobic and have been predicted to be largely α-helical proteins that readily oligomerize. Third, viroporins contain an amphipathic α-helix that forms the aqueous channel. Therefore, we can reasonably speculate that the 2B protein is a viroporin protein.

Transmembrane Mode of the 2B Protein in DEF Cells

To further explore the membrane topology of the 2B protein in DEF cells, HA and FLAG tags were added to the C-terminus and the N-terminus of the 2B protein, respectively, to construct the eukaryotic expression vectors pCAGGS-2B-HA and pCAGGS-FLAG-2B. The Western blotting (**WB**) results showed that a specific band appeared below 15 kilodaltons (**kDa**), which was consistent with the predicted size, proving that the fusion proteins 2B-HA (Figure 2A) and FLAG-2B (Figure 2B) were correctly expressed and could be used in subsequent experiments.

When cells are treated with Triton X-100, the rabbit anti-HA or FLAG antibody can enter the cells and organelles and the antibody can bind to the antigen facing the cytoplasmic matrix and the organelle simultaneously. After the cells are treated with digitonin, the antibody cannot enter the organelle and it can bind to only the antigen facing the cytoplasmic matrix. Red fluorescence was observed in pCAGGS-2B-HA and pCAGGS-FLAG-2B cells treated with Triton X-100 (Figure 3), and only pCAGGS-2B-HA exhibited red fluorescence when the cells were treated with digitonin. This indicates that the HA tag is oriented toward the cytoplasmic matrix, and since the HA tag is located at the C-terminus of the 2B protein. This result indicates that the C-terminus of the 2B protein faces the cytoplasmic matrix, and the N-terminus faces the organelle lumen. This transmembrane manner is consistent with viroporin type IA.

Changes in The Ca2+Concentration in DEF Cells

In this study, the fluorescent probe Fluo-3 AM was used to detect changes in Ca2+ concentration in the host cytoplasm after expression of the 2B protein. Fluo-3 AM is a fluorescent probe that can penetrate the cell membrane. After entering the cell, it can be cleaved by intracellular esterases to form Fluo-3, which is then retained in the cell. Fluo-3 can combine with Ca2+ to generate strong fluorescence, with a maximum excitation wavelength of 488 nm and a maximum emission wavelength of 526 nm. Therefore, the fluorescence intensity can reflect the concentration of cytoplasmic Ca2+. As shown in Figure 4, the fluorescence of the transfected pCAGGS-2B-HA group was upregulated ($P = 0.001$) compared with that of the empty-loaded pCAGGS group, which indicated that the expression of the 2B protein caused the intracellular Ca2+ concentration to rise.

Autophagy Induced by the 2B Protein in DEF Cells

Ca2+ participates in the regulation of many physiological processes in cells, such as autophagy and apoptosis. Next, we examined the level of the LC3 protein to monitor the autophagy process by Western blotting. As shown in Figure 5A, rapamycin treatment resulted in the upregulation of LC3-II compared with the pCAGGS group, and the transfection expression in the 2B protein group was similar. We further analyzed the gray value of the WB results (Figure 5B), and the results showed that there was a difference ($P = 0.01$) between the 2B groups and the pCAGGS group and a difference ($P = 0.02$) between the rapamycin group and the pCAGGS group.

Moreover, we also detected the effects of the 2B protein on autophagy with the green single fluorescent indicator system GFP-LC3. As shown in Figure 5C, the green fluorescence of the GFP-LC3 fusion protein in the pCAGGS group was uniformly distributed in the cytoplasm, while in the 2B protein and rapamycin treatment groups showed green fluorescent spots, indicating that the expression of the 2B protein caused the

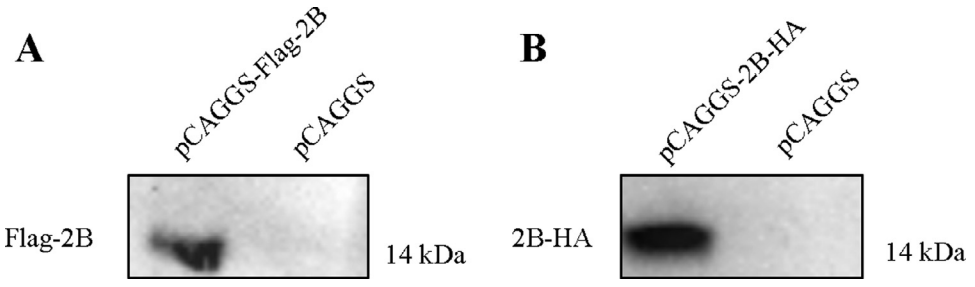

Figure 2. Expression analysis of eukaryotic recombinant plasmid. (A) The pCAGGS-2B-HA plasmid (4.0 μg) were transfected into duck embryo fibroblasts (DEF) cells. Cell lysates were collected at 48-h post-transfection and analyzed by immunoblot using indicated antibodies. (B) The pCAGGS-Flag-2B plasmid (4.0 μg) was transfected into DEF cells. Cell lysates were collected at 48-h post-transfection and analyzed by immunoblot using indicated antibodies.

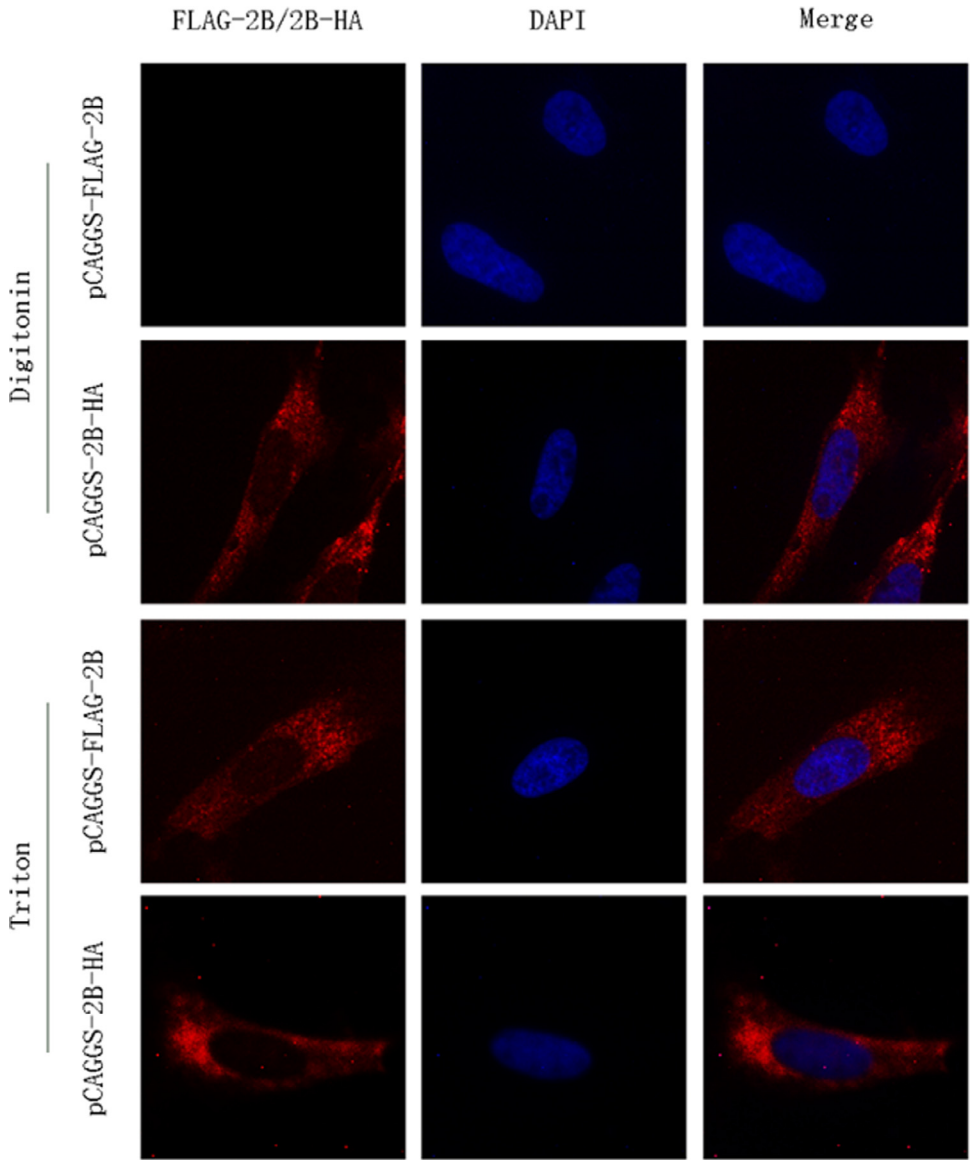

Figure 3. Membrane topology of the 2B protein in Duck embryo fibroblasts (DEF) cells. The pCAGGS-2B-HA (4.0 μg) or pCAGGS-Flag-2B plasmid (4.0 μg) were transfected into DEF cells. The Digitonin group was permeabilized with digitalis saponin (0.01 mg / mL); the Triton group was permeabilized with 0.25% Triton-100. The blue fluorescence represents the nucleus and the red fluorescence represents the target protein. Images were captured by fluorescence microscopy using a 40× objective.

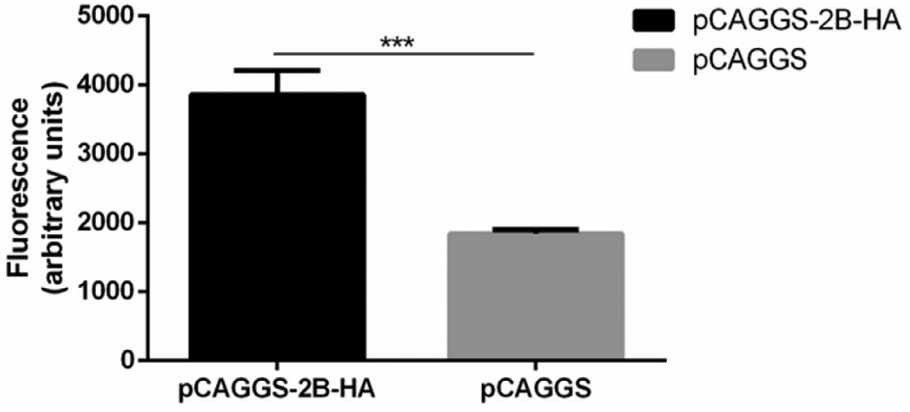

Figure 4. Effect of 2B protein on cytosolic calcium concentration in host cells. The pCAGGS-2B-HA (4.0 μg) or pCAGGS plasmid (4.0 μg) were transfected into duck embryo fibroblasts (DEF) cells. Then the cells were stained with Fluo-3 AM at 48-h post-transfection. A histogram was constructed to reveal the changes in the intracellular Ca^{2+}concentration. Differences between two groups were analyzed using Student's t test and were considered significant at * $P < 0.05$, ** $P < 0.01$, *** $P < 0.001$.

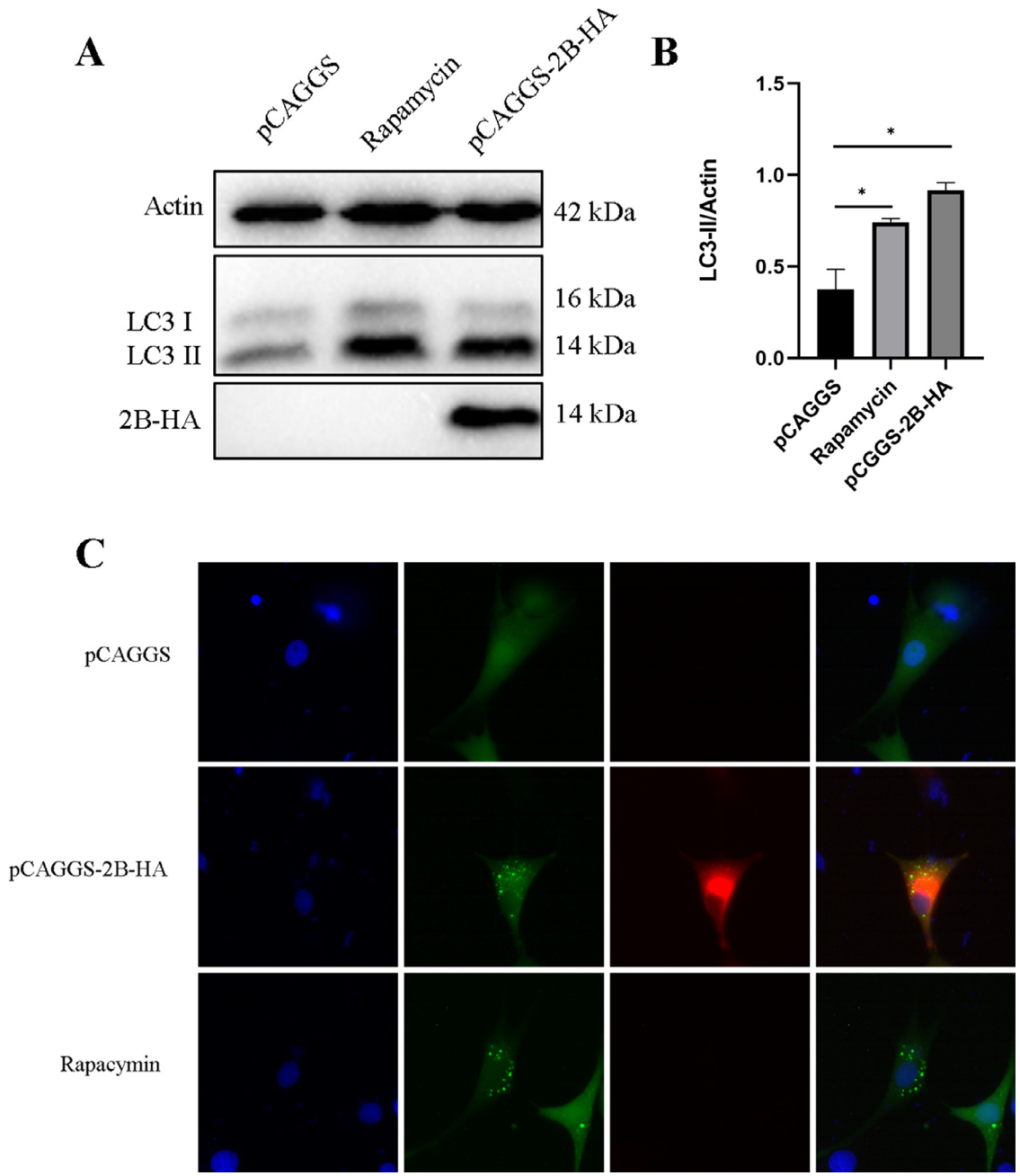

Figure 5. Autophagy induced by the 2B protein in Duck embryo fibroblasts (DEF) cells. (A, C) The GFP-LC3 plasmid (2.0 μg) was transfected into DEF cells. One group was cotransfected with 2.0 μg of pCAGGS-2B-HA, another group was cotransfected with 2.0 μg of the pCAGGS empty vector as a negative control, and the last group was added with rapamycin (100 nM) 4 h before harvest as a positive control. (A) The microtubule-associated protein 1 light chain 3 II (**LC3-II**) levels were determined by Western blot analysis with an anti-LC3 antibody. (B) Band intensity was quantified using ImageJ, and β-actin was used as a loading control. The ratio of LC3-II to β-actin was normalized to the pCAGGS empty vector group. Differences between two groups were analyzed using Student's t test and were considered significant at * $P < 0.05$, ** $P < 0.01$, *** $P < 0.001$. (C) Cell slides were collected at 48-h post-transfection and stained with 4′,6-diamidino-2-phenylindole (DAPI) after fixation and permeation. The results were observed with a fluorescence microscope after glycerol fixation. Blue fluorescence represents the nucleus, green fluorescence represents autophagosomes, and red fluorescence represents the 2B protein. Images were captured by fluorescence microscopy using a 40× objective.

accumulation of autophagosomes. These results indicated that the expression of the 2B protein causes autophagy.

Effect Of 2B Protein on Autophagic Flow

When the autophagic flow is complete, autophagy substrates such as the protein sequestosome 1 (**SQSTM1/p62**) will be degraded, so reduction of the p62 protein can be used as a marker for the completion of autophagy. As shown in Figures 6A and 6B, the protein content of p62 was higher ($P = 0.014$) in the mock group, and degradation of the p62 protein in the rapamycin treatment group was greater than that in the 2B group ($P = 0.023$). Gray value analysis further showed that compared with the pCAGGS empty vector group, the amount of p62 in the 2B transfection group was

58.7%, and the amount of p62 in the rapamycin group was 43.2%. Therefore, the decrease in p62 levels was not as sharp as that in the positive control group but more than that in the empty pCAGGS group. The results showed that the autophagic flow of the 2B protein group was not as complete as that of the positive control group.

We also investigated the effects of the 2B protein on autophagy flow by using the mRFP-GFP-LC3 dual fluorescent indicator system and observing the colocalization of autophagosomes and lysosomes. As shown in Figure 6C, the mock group did not show obvious fluorescent spots, while in the starvation and rapamycin treatment groups, red fluorescent spots appeared, and in the 2B transfection group, both green fluorescent spots and red fluorescent spots appeared and were rendered orange. These results indicated that autofluorescence from green fluorescent dot quenching occurred in the starvation and rapamycin treatment groups, while expression of the 2B protein caused autophagy of the host DEF cells but inhibited the combination of the autophagosome and endosomes, so the autophagosomes appeared orange. In Figure 6D, red indicates lysosomal staining, and the dots formed by the aggregation of the green fluorescent protein GFP-LC3 represent autophagosomes. The green fluorescent protein in the rapamycin and starvation treatment groups partially overlapped with the lysosomes, while the green fluorescent protein in the 2B transfection group did not overlap with the lysosomes. This further demonstrates that the 2B protein blocks autophagic flow by inhibiting the binding of autophagosomes to lysosomes.

DISCUSSION

Autophagy is a catabolic cellular process involving an intracellular membrane trafficking pathway that is important for recycling cellular components or eliminating intracellular microbes in lysosomes. In general,

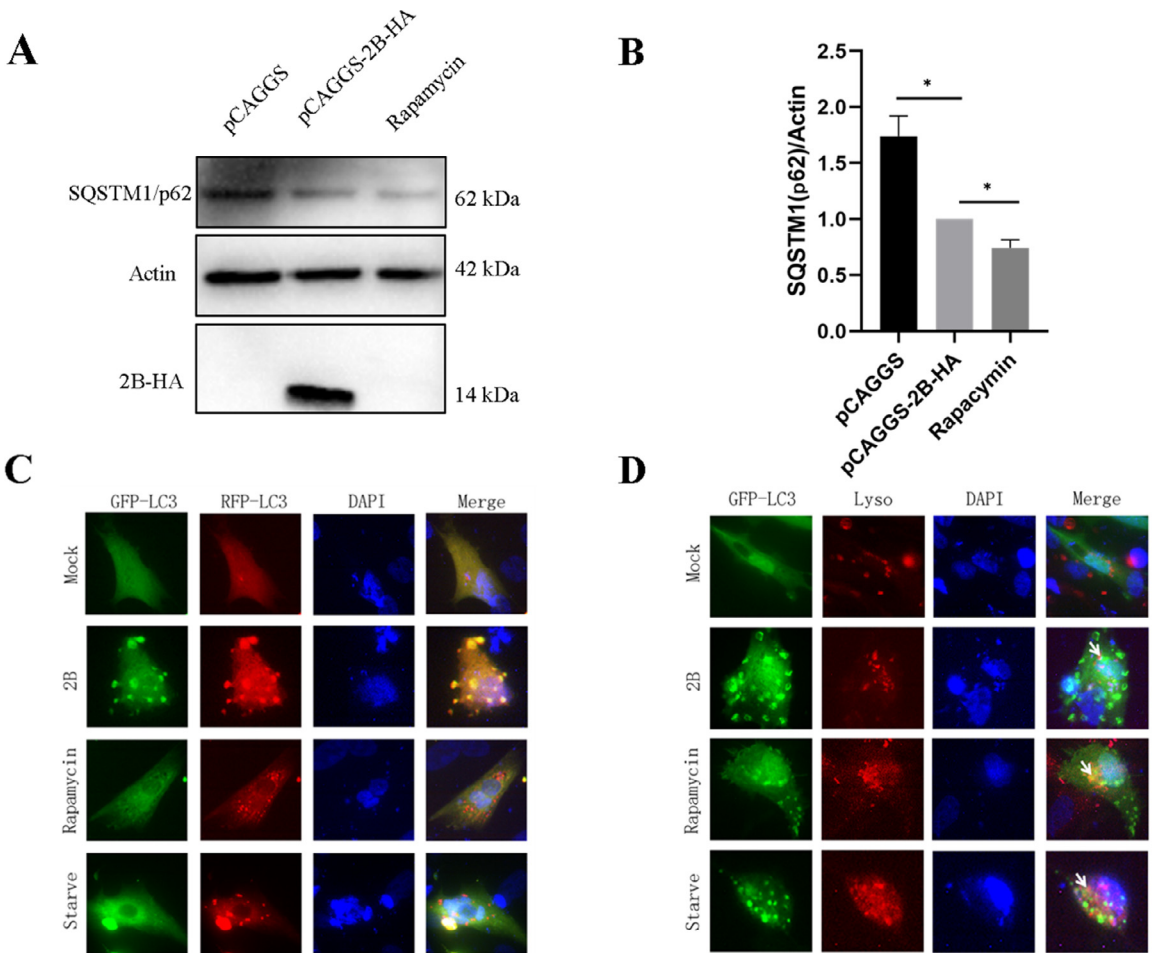

Figure 6. Effect of 2B protein on autophagic flow. (A, D) The GFP-LC3 plasmid (2.0 μg) was transfected into duck embryo fibroblasts (DEF) cells. The rapamycin and starve groups were used as positive controls, and the pCAGGS empty group was used as negative controls. (A) One group was cotransfected with 2.0 μg of pCAGGS-2B-HA, another group was cotransfected with 2.0 μg of the pCAGGS empty vector and the p62 protein levels were determined by Western blot analysis with an anti-SQSTM1/p62 antibody. (B) Band intensity was quantified using ImageJ, and β-actin was used as a loading control. The ratio of SQSTM1/p62 to β-actin was normalized to the pCAGGS-2B-HA group. Differences between two groups were analyzed using Student's t-test and were considered significant at * $P < 0.05$, ** $P < 0.01$, *** $P < 0.001$. (C) Double fluorescence mRFP-GFP-LC3 indicator system to detect whether autophagosomes are fused to lysosomes. Images were captured by fluorescence microscopy using a 40× objective. (D) Lysosomal staining to detect colocalization of autophagosomes and lysosomes. Blue fluorescence represents the nucleus, green fluorescence represents the LC3 protein, and red fluorescence represents lysosomes. White arrows indicate the colocalization status of autophagosomes and lysosomes in different treatment groups. Images were captured by fluorescence microscopy using a 40× objective.

autophagy plays an important role in initiating the innate and adaptive immunity responses of host cells to clear viral and bacterial infections, but studies have shown that viruses can also use the autophagy pathway to promote self-replication (Abernathy et al., 2019). Rotavirus hijacks autophagy by calcium/calmodulin-dependent kinase-β signaling activated by viroporin NSP4 to promote virus replication (Crawford et al., 2012b). Our experiments herein show that the DHAV-1 2B protein has viroporin-like properties, can mediate Ca2+ permeability and lead to increased cytosolic calcium, and the 2B protein transmembrane mode is the same as that for type IA viroporins (Figures 3 and 4). Although it belongs to the picornavirus family, the transmembrane modes of poliovirus (**PV**), CBV and the FMDV 2B protein are consistent with the viroporin type II, which is an interesting phenomenon (Agirre et al., 2002; Nieva et al., 2003; Ao et al., 2015). Although the DHAV-1 2B protein contains only one transmembrane region different from other picornavirus (Figure 1), the 2B protein works by forming a transmembrane channel through oligomerization of the monomer, so the effects on its biological function may not be obvious (Ao et al., 2015).

The 2B protein induced a significant increase in the Ca2+ concentration in the cytoplasm of the host (Figure 4), but it has not yet been determined whether the Ca2+ originated from an extracellular Ca2+ influx or due to Ca2+ outflow from organelles. Rotavirus viroporin NSP4 localizes to the ER and rapidly induces Ca2+ influx through the plasma membrane, which researchers initially thought was a cellular process termed capacitive calcium entry (Putney, 1986). This process was later renamed store-operated calcium entry (**SOCE**). The specific mechanism is that a decrease in ER Ca2+ will cause Ca2+ to dissociate from EF-hand, thereby triggering stromal interaction molecule 1 (**STIM1**) to oligomerize. The STIM1 oligomer moves to the plasma membrane and activates the Orai1 channel thereon, and extracellular Ca2+ flows into the cell and balances the Ca2+ storage in the ER (Soboloff et al., 2012). However, further work is needed to determine whether STIM1 or Orai1 in the SOCE molecular mechanism is activated by DHAV-1 2B. Studies have demonstrated that the picornavirus 2B protein inhibits protein transport by localizing to the Golgi apparatus to reduce Ca2+ levels in the ER/Golgi apparatus, whereas when the 2B protein is localized in only the ER, the 2B protein multimers are insufficient to form transmembrane pores, Ca2+ levels in the ER/Golgi matrix cannot be reduced and protein transport cannot be inhibited (de Jong et al., 2003; de Jong et al., 2006). This may be due to the different lipid compositions between the ER membrane and the Golgi membrane, which affects the structure of the 2B protein multimer and leads to differences in its effects on Ca2+ concentration, which ultimately leads to functional differences. In addition, this inhibition of the protein transport pathway may also be because viral proteins change the ion conditions in the Golgi cavity through their viroporin properties, thereby inhibiting the sugar-modifying enzyme in the Golgi complex (de Jong et al., 2006). Consistent with this, poliovirus 2B was reported to accumulate secretory glycoproteins in an endoglycosidase H-sensitive glycosylation state (Doedens and Kirkegaard, 1995).

Next, we confirmed by WB of LC3 (Figure 5A) and the GFP-LC3 single fluorescent indicator system (Figure 5C) that DHAV-1 2B protein expression caused a significant increase in LC3-II and the accumulation of autophagosomes, demonstrating that the expression of the 2B protein can induce the development of autophagy, which is consistent with the previously reported CVB 2B protein-induced autophagy (Wu et al., 2016). Later, we detected the autophagy degradation substrate protein SQSTM1/p62 by WB, and indirect immunofluorescence experiments confirmed that the 2B protein blocked the complete occurrence of autophagy flow by blocking the fusion of autophagosomes to lysosomes/endosomes (Figure 6). These results are consistent with existing reports that picornaviruses induce autophagy in host cells and block the completion of autophagic flow by inhibiting the fusion of autophagosomes with lysosomes (Shi et al., 2016; Corona et al., 2018; Mohamud et al., 2018). Previous studies have shown that many picornaviruses can rely on intracellular membrane structures for replication, such as the ER, Golgi, and mitochondrial membranes. For the virus itself, complete autophagy of the host cell will cause its genetic material and protein to be degraded, so inhibition of the completion of the autophagic flow will also prevent the virus from being cleared by autophagy (Kimura et al., 2017). It seems that the induced autophagy of the virus but hindrance of the autophagic flow is of great significance for its own replication and transmission. In fact, there is evidence that a variety of picornaviruses, such as enterovirus 71 (**EV71**) and CVB, can assist in self-replication by manipulating the autophagy process (Huang et al., 2009). The inhibition of autophagic flow by the virus leads to the accumulation of autophagosomes, which may lead to blocking of the transport and circulation of intracellular vesicles. These stacked membrane structures may provide a replication site for the virus and greatly promote the replication and synthesis of viruses (Gannage et al., 2009a; McLean et al., 2011a; Crawford et al., 2012a). Furthermore, studies have shown that after replication of the virus in autophagosomes, microvesicles (**EMVs**) are formed and leave the cell to complete nonlytic propagation (Bird et al., 2014; Robinson et al., 2014; Chen et al., 2015).

Studies have shown that the effect of certain viruses on autophagy in host cells may be caused by increased Ca2+ concentration in the cytoplasm. Rotavirus-initiated autophagy involves ER-localized NSP4 releasing ER calcium to increase cytoplasmic Ca2+ concentrations, thereby activating Ca2+/calmodulin-dependent protein kinase kinase β (**CaMKK-β**), which phosphorylates adenosine 5'-monophosphate (**AMP**)-activated protein kinase (**AMPK**) to initiate autophagy (Crawford et al., 2012b). Chelation of cytoplasmic Ca2+ or expression of the viroporin-defective NSP4 mutant

abrogates the induction of autophagy, indicating that this is a viroporin-mediated autophagy pathway (Crawford and Estes, 2013). Therefore, we can reasonably speculate that the DHAV-1 2B protein causes autophagy by enhancing the permeability of the cell membrane structure and causing an imbalance in intracellular Ca2+, but this signaling pathway remains to be further explored.

In conclusion, our findings greatly expand our understanding of the function of the DHAV-1 nonstructural protein 2B and the pathogenicity of the virus. DHAV-1 causes internal ionic disorders and affects the autophagy process of host cells through its nonstructural protein 2B. Because viruses may promote their own replication by affecting the process of autophagy, a better understanding of the relationship between viruses and host cell autophagy can help develop new therapeutic strategies to treat viral infections and related diseases.

ACKNOWLEDGMENTS

This work was supported by China Agricultural Research System of MOF and MARA, the Sichuan Veterinary Medicine and Drug Innovation Group of China Agricultural Research System (SCCXTD-2021-18).

DISCLOSURES

The authors declare that they have no conflict of interest.

REFERENCES

Abernathy, E., R. Mateo, K. Majzoub, N. van Buuren, S. W. Bird, J. E. Carette, and K. Kirkegaard. 2019. Differential and convergent utilization of autophagy components by positive-strand RNA viruses. PLoS Biol. 17:e2006926.

Agirre, A., A. Barco, L. Carrasco, and J. L. Nieva. 2002. Viroporin-mediated membrane permeabilization. Pore formation by nonstructural poliovirus 2B protein. J. Biol. Chem. 277:40434–40441.

Ao, D., H. C. Guo, S. Q. Sun, D. H. Sun, T. S. Fung, Y. Q. Wei, S. C. Han, X. P. Yao, S. Z. Cao, D. X. Liu, and X. T. Liu. 2015. Viroporin activity of the foot-and-mouth disease virus non-structural 2B protein. PLoS One 10:e0125828.

Bagchi, P., D. Dutta, S. Chattopadhyay, A. Mukherjee, U. C. Halder, S. Sarkar, N. Kobayashi, S. Komoto, K. Taniguchi, and M. Chawla-Sarkar. 2010. Rotavirus nonstructural protein 1 suppresses virus-induced cellular apoptosis to facilitate viral growth by activating the cell survival pathways during early stages of infection. J. Virol. 84:6834–6845.

Bird, S. W., N. D. Maynard, M. W. Covert, and K. Kirkegaard. 2014. Nonlytic viral spread enhanced by autophagy components. PNAS 111:13081–13086.

Buchan, D. W. A., and D. T. Jones. 2019. The PSIPRED protein analysis workbench: 20 years on. Nucl. Acids. Res. 47:W402–W407.

Chen, Y. H., W. L. Du, M. C. Hagemeijer, P. M. Takvorian, C. Pau, A. Cali, C. A. Brantner, E. S. Stempinski, P. S. Connelly, H. C. Ma, P. Jiang, E. Wimmer, G. Altan-Bonnet, and N. Altan-Bonnet. 2015. Phosphatidylserine vesicles enable efficient en bloc transmission of enteroviruses. Cell 160:619–630.

Cheng, A. C., M. S. Wang, H. Y. Xin, D. K. Zhu, X. R. Li, H. J. Chen, R. Y. Jia, and M. A. Yang. 2009. Development and application of a reverse transcriptase polymerase chain reaction to detect Chinese isolates of duck hepatitis virus type 1 (vol 76, pg 1, 2009). J. Microbiol. Methods 77:331.

Corona, A. K., H. M. Saulsbery, A. F. Corona Velazquez, and W. T. Jackson. 2018. Enteroviruses remodel autophagic trafficking through regulation of host SNARE proteins to promote virus replication and cell exit. Cell Rep. 22:3304–3314.

Crawford, S. E., J. M. Hyser, B. Utama, and M. K. Estes. 2012b. Autophagy hijacked through viroporin-activated calcium/calmodulin-dependent kinase kinase-beta signaling is required for rotavirus replication. Proc. Natl. Acad. Sci. U. S. A. 109:E3405–E3413.

Crawford, S. E., and M. K. Estes. 2013. Viroporin-mediated calcium-activated autophagy. Autophagy 9:797–798.

de Jong, A. S., E. Wessels, H. B. Dijkman, J. M. Galama, W. J. Melchers, P. H. Willems, and F. J. van Kuppeveld. 2003. Determinants for membrane association and permeabilization of the coxsackievirus 2B protein and the identification of the Golgi complex as the target organelle. J. Biol. Chem. 278:1012–1021.

de Jong, A. S., H. J. Visch, F. de Mattia, M. M. van Dommelen, H. G. Swarts, T. Luyten, G. Callewaert, W. J. Melchers, P. H. Willems, and F. J. van Kuppeveld. 2006. The coxsackievirus 2B protein increases efflux of ions from the endoplasmic reticulum and Golgi, thereby inhibiting protein trafficking through the Golgi. J. Biol. Chem. 281:14144–14150.

Ding, C., and D. Zhang. 2007. Molecular analysis of duck hepatitis virus type 1. Virology 361:9–17.

Doedens, J. R., and K. Kirkegaard. 1995. Inhibition of cellular protein secretion by poliovirus proteins 2B and 3A. EMBO J. 14:894–907.

Gannage, M., D. Dormann, R. Albrecht, J. Dengjel, T. Torossi, P. C. Ramer, M. Lee, T. Strowig, F. Arrey, G. Conenello, M. Pypaert, J. Andersen, A. Garcia-Sastre, and C. Munz. 2009a. Matrix protein 2 of influenza A virus blocks autophagosome fusion with lysosomes. Cell Host Microbe 6:367–380.

Gannage, M., D. Dormann, R. Albrecht, J. Dengjel, T. Torossi, P. C. Ramer, M. Lee, T. Strowig, F. Arrey, G. Conenello, M. Pypaert, J. Andersen, A. Garcia-Sastre, and C. Munz. 2009b. Matrix protein 2 of influenza A virus blocks autophagosome fusion with lysosomes. Cell Host Microbe 6:367–380.

Giorda, K. M., and D. N. Hebert. 2013. Viroporins customize host cells for efficient viral propagation. DNA Cell Biol. 32:557–564.

Gonzalez, M. E., and L. Carrasco. 2003. Viroporins. FEBS Lett. 552:28–34.

Guo, H. C., Y. Jin, X. Y. Zhi, D. Yan, and S. Q. Sun. 2015. NLRP3 inflammasome activation by viroporins of animal viruses. Viruses 7:3380–3391.

Haijun, C., C. Anchun, W. Minghsu, Z. Dekang, Y. Miao, Z. Yi, and C. Xiaoyue. 2007. Isolation and identification of the pathogen of duck virus hepatitis. China Poultry 29:13–16.

Heng, W., Z. Xia, C. Yang, W. Ruixue, L. Lexun, C. Sijia, W. Tianying, Z. Xiaoyan, W. Xiaoyu, W. Yan, Z. Fengmin, Z. Wenran, and Z. Zhaohua. 2016. Protein 2B of Coxsackievirus B3 induces autophagy relying on its transmembrane hydrophobic sequences. Viruses 8:131.

Hu, Q., D. K. Zhu, G. P. Ma, A. Cheng, M. S. Wang, S. Chen, R. Y. Jia, M. F. Liu, K. F. Sun, Q. Yang, Y. Wu, and X. Y. Chen. 2016. A one-step duplex rRT-PCR assay for the simultaneous detection of duck hepatitis A virus genotypes 1 and 3. J. Virol. Methods 236:207–214.

Huang, S. C., C. L. Chang, P. S. Wang, Y. Tsai, and H. S. Liu. 2009. Enterovirus 71-induced autophagy detected in vitro and in vivo promotes viral replication. J. Med. Virol. 81:1241–1252.

Hyser, J. M., and M. K. Estes. 2015. Pathophysiological consequences of calcium-conducting viroporins. Annu. Rev. Virol. 2:473–496.

Kim, M. C., Y. K. Kwon, S. J. Joh, A. M. Lindberg, J. H. Kwon, J. H. Kim, and S. J. Kim. 2006. Molecular analysis of duck hepatitis virus type 1 reveals a novel lineage close to the genus Parechovirus in the family Picornaviridae. J. Gen. Virol. 87:3307–3316.

Kimura, T., J. Y. Jia, S. Kumar, S. W. Choi, Y. X. Gu, M. Mudd, N. Dupont, S. Y. Jiang, R. Peters, F. Farzam, A. Jain, K. A. Lidke, C. M. Adams, T. Johansen, and V. Deretic. 2017. Dedicated SNAREs and specialized TRIM cargo receptors mediate secretory autophagy. EMBO J. 36:42–60.

Lai, Y., N. Zeng, M. Wang, A. Cheng, Q. Yang, Y. Wu, R. Jia, D. Zhu, X. Zhao, S. Chen, M. Liu, S. Zhang, Y. Wang, Z. Xu, Z. Chen, L. Zhu, Q. Luo, Y. Liu, Y. Yu, L. Zhang, J. Huang, B. Tian, L. Pan, M. Ur Rehman, and X. Chen. 2019. The VP3 protein of duck hepatitis A virus mediates host cell adsorption and apoptosis. Sci. Rep. 9:16783.

Lamb, C. A., H. C. Dooley, and S. A. Tooze. 2013. Endocytosis and autophagy: shared machinery for degradation. Bioessays 35:34–45.

Landajuela, A., J. H. Hervas, Z. Anton, L. R. Montes, D. Gil, M. Valle, J. F. Rodriguez, F. M. Goni, and A. Alonso. 2016. Lipid geometry and bilayer curvature modulate LC3/GABARAP-mediated model autophagosomal elongation. Biophys. J. 110:411–422.

Levine, B., and G. Kroemer. 2008. Autophagy in the pathogenesis of disease. Cell 132:27–42.

Levine, B., N. Mizushima, and H. W. Virgin. 2011. Autophagy in immunity and inflammation. Nature 469:323–335.

Luis Nieva, J., and L. Carrasco. 2015. Viroporins: structures and functions beyond cell membrane permeabilization. Viruses 7:5169–5171.

Mao, S., X. Ou, D. Zhu, S. Chen, G. Ma, M. Wang, R. Jia, M. Liu, K. Sun, Q. Yang, Y. Wu, X. Chen, and A. Cheng. 2016. Development and evaluation of indirect ELISAs for the detection of IgG, IgM and IgA1 against duck hepatitis A virus 1. J. Virol. Methods 237:79–85.

Mao, S., M. Wang, X. Ou, D. Sun, A. Cheng, D. Zhu, S. Chen, R. Jia, M. Liu, K. Sun, Q. Yang, Y. Wu, X. Zhao, and X. Chen. 2017. Virologic and immunologic characteristics in mature ducks with acute duck hepatitis A virus 1. Infection. Front Immunol. 8:1574.

McLean, J. E., A. Wudzinska, E. Datan, D. Quaglino, and Z. Zakeri. 2011a. Flavivirus NS4A-induced autophagy protects cells against death and enhances virus replication. J. Biol. Chem. 286:22147–22159.

McLean, J. E., A. Wudzinska, E. Datan, D. Quaglino, and Z. Zakeri. 2011b. Flavivirus NS4A-induced autophagy protects cells against death and enhances virus replication. J. Biol. Chem. 286:22147–22159.

Mohamud, Y., J. Shi, J. Qu, T. Poon, Y. C. Xue, H. Deng, J. Zhang, and H. Luo. 2018. Enteroviral infection inhibits autophagic flux via disruption of the SNARE complex to enhance viral replication. Cell Rep. 22:3292–3303.

Monika, J., P. Christian, and G. M. Verena. 1998. Membrane permeability induced by hepatitis A virus proteins 2B and 2BC and proteolytic processing of HAV 2BC. Virology 252:218–227.

Nakatogawa, H. 2013. Two ubiquitin-like conjugation systems that mediate membrane formation during autophagy. Essays Biochem. 55:39–50.

Ni, H. M., A. Bockus, A. L. Wozniak, K. Jones, S. Weinman, X. M. Yin, and W. X. Ding. 2011. Dissecting the dynamic turnover of GFP-LC3 in the autolysosome. Autophagy 7:188–204.

Nieva, J. L., A. Agirre, S. Nir, and L. Carrasco. 2003. Mechanisms of membrane permeabilization by picornavirus 2B viroporin. FEBS Lett. 552:68–73.

Nieva, J. L., V. Madan, and L. Carrasco. 2012. Viroporins: structure and biological functions. Nat. Rev. Microbiol. 10:563–574.

Ou, X., S. Mao, Y. Jiang, S. Zhang, C. Ke, G. Ma, A. Cheng, M. Wang, D. Zhu, S. Chen, R. Jia, M. Liu, K. Sun, Q. Yang, Y. Wu, and X. Chen. 2017a. Viral-host interaction in kidney reveals strategies to escape host immunity and persistently shed virus to the urine. Oncotarget 8:7336–7349.

Ou, X., S. Mao, J. Cao, A. Cheng, M. Wang, D. Zhu, S. Chen, R. Jia, M. Liu, K. Sun, Q. Yang, Y. Wu, and X. Chen. 2017b. Comparative analysis of virus-host interactions caused by a virulent and an attenuated duck hepatitis A virus genotype 1. PLoS One 12: e0178993.

Ou, X., S. Mao, J. Cao, Y. Ma, G. Ma, A. Cheng, M. Wang, D. Zhu, S. Chen, R. Jia, M. Liu, K. Sun, Q. Yang, Y. Wu, and X. Chen. 2017c. The neglected avian hepatotropic virus induces acute and chronic hepatitis in ducks: an alternative model for hepatology. Oncotarget 8:81838–81851.

Ou, X., M. Wang, S. Mao, J. Cao, A. Cheng, D. Zhu, S. Chen, R. Jia, M. Liu, Q. Yang, Y. Wu, X. Zhao, S. Zhang, Y. Liu, Y. Yu, L. Zhang, X. Chen, M. P. Peppelenbosch, and Q. Pan. 2018. Incompatible translation drives a convergent evolution and viral attenuation during the development of live attenuated vaccine. Front. Cell Infect. Microbiol. 8:249.

Putney, J. W. Jr. 1986. A model for receptor-regulated calcium entry. Cell Calcium 7:1–12.

Robinson, S. M., G. Tsueng, J. Sin, V. Mangale, S. Rahawi, L. L. McIntyre, W. Williams, N. Kha, C. Cruz, B. M. Hancock, D. P. Nguyen, M. R. Sayen, B. J. Hilton, K. S. Doran, A. M. Segall, R. Wolkowicz, C. T. Cornell, J. L. Whitton, R. A. Gottlieb, and R. Feuer. 2014. Coxsackievirus B Exits the host cell in shed microvesicles displaying autophagosomal markers. PLoS Pathog. 10:e1004045.

Saier, M. H. Jr., C. V. Tran, and R. D. Barabote. 2006. TCDB: the Transporter Classification Database for membrane transport protein analyses and information. Nucl. Acids. Res. 34: D181–D186.

Shan, Z., C. Anchun, and W. Mingshu. 2017. The autophagy in Picornavirus infection. Chinese Journal of Cell Biology 39:1619–1625.

Shen, Y. L., A. C. Cheng, M. S. Wang, S. Chen, R. Y. Jia, D. K. Zhu, M. F. Liu, K. F. Sun, Q. Yang, and X. Y. Chen. 2015. Development of an indirect ELISA method based on the VP3 protein of duck hepatitis A virus type 1 (DHAV-1) for dual detection of DHAV-1 and DHAV-3 antibodies. J. Virol. Methods 225:30–34.

Shi, X., Z. Chen, S. Tang, F. Wu, S. Xiong, and C. Dong. 2016. Coxsackievirus B3 infection induces autophagic flux, and autophagosomes are critical for efficient viral replication. Arch. Virol. 161:2197–2205.

Soboloff, J., B. S. Rothberg, M. Madesh, and D. L. Gill. 2012. STIM proteins: dynamic calcium signal transducers. Nat. Rev. Mol. Cell Biol. 13:549–565.

Song, C., S. Yu, Y. Duan, Y. Hu, X. Qiu, L. Tan, Y. Sun, M. Wang, A. Cheng, and C. Ding. 2014. Effect of age on the pathogenesis of DHV-1 in Pekin ducks and on the innate immune responses of ducks to infection. Arch. Virol. 159:905–914.

Sun, D., M. Wang, X. Wen, A. Cheng, R. Jia, K. Sun, Q. Yang, Y. Wu, D. Zhu, S. Chen, M. Liu, X. Zhao, and X. Chen. 2017. Cleavage of poly(A)-binding protein by duck hepatitis A virus 3C protease. Sci. Rep. 7:16261.

Sun, D., X. Wen, M. Wang, S. Mao, A. Cheng, X. Yang, R. Jia, S. Chen, Q. Yang, Y. Wu, D. Zhu, M. Liu, X. Zhao, S. Zhang, Y. Wang, Z. Xu, Z. Chen, L. Zhu, Q. Luo, Y. Liu, Y. Yu, L. Zhang, and X. Chen. 2019a. Apoptosis and autophagy in Picornavirus infection. Front. Microbiol. 10:2032.

Sun, D., M. Wang, X. Wen, S. Mao, A. Cheng, R. Jia, Q. Yang, Y. Wu, D. Zhu, S. Chen, M. Liu, X. Zhao, S. Zhang, X. Chen, Y. Liu, Y. Yu, and L. Zhang. 2019b. Biochemical characterization of recombinant Avihepatovirus 3C protease and its localization. Virol. J 16:54.

Tseng, C. H., N. J. Knowles, and H. J. Tsai. 2007. Molecular analysis of duck hepatitis virus type 1 indicates that it should be assigned to a new genus. Virus Res. 123:190–203.

Wen, X., A. Cheng, M. Wang, R. Jia, D. Zhu, S. Chen, M. Liu, K. Sun, Q. Yang, Y. Wu, and X. Chen. 2015. Recent advances from studies on the role of structural proteins in enterovirus infection. Fut. Microbiol. 10:1529–1542.

Wen, X., D. Zhu, A. Cheng, M. Wang, S. Chen, R. Jia, M. Liu, K. Sun, X. Zhao, Q. Yang, Y. Wu, and X. Chen. 2018. Molecular epidemiology of duck hepatitis a virus types 1 and 3 in China, 2010-2015. Transbound Emerg. Dis. 65:10–15.

Wen, X. J., A. C. Cheng, M. S. Wang, R. Y. Jia, D. K. Zhu, S. Chen, M. F. Liu, F. Liu, and X. Y. Chen. 2014. Detection, differentiation, and VP1 sequencing of duck hepatitis A virus type 1 and type 3 by a 1-step duplex reverse-transcription PCR assay. Poult. Sci. 93:2184–2192.

Wu, H., X. Zhai, Y. Chen, R. Wang, L. Lin, S. Chen, T. Wang, X. Zhong, X. Wu, Y. Wang, F. Zhang, W. Zhao, and Z. Zhong. 2016. Protein 2B of Coxsackievirus B3 induces autophagy relying on its transmembrane hydrophobic sequences. Viruses 8:131.

Wu, X., R. Jia, M. Wang, S. Chen, M. Liu, D. Zhu, X. Zhao, Q. Yang, Y. Wu, Z. Yin, S. Zhang, J. Huang, L. Zhang, Y. Liu, Y. Yu, L. Pan, B. Tian, M. U. Rehman, X. Chen, and A. Cheng. 2019. Downregulation of microRNA-30a-5p contributes to the replication of duck enteritis virus by regulating Beclin-1-mediated autophagy. Virol J 16:144.

Xie, J., Q. Zeng, M. Wang, X. Ou, Y. Ma, A. Cheng, X. X. Zhao, M. Liu, D. Zhu, S. Chen, R. Jia, Q. Yang, Y. Wu, S. Zhang, Y. Liu, Y. Yu, L. Zhang, and X. Chen. 2018a. Transcriptomic characterization of a chicken embryo model infected with duck hepatitis A virus type 1. Front. Immunol. 9:1845.

Xie, J., M. Wang, A. Cheng, X. X. Zhao, M. Liu, D. Zhu, S. Chen, R. Jia, Q. Yang, Y. Wu, S. Zhang, Y. Liu, Y. Yu, L. Zhang, K. Sun, and X. Chen. 2018b. Cytokine storms are primarily

responsible for the rapid death of ducklings infected with duck hepatitis A virus type 1. Sci. Rep. 8:6596.

Xie, J., M. Wang, A. Cheng, X. X. Zhao, M. Liu, D. Zhu, S. Chen, R. Jia, Q. Yang, Y. Wu, S. Zhang, Y. Liu, Y. Yu, L. Zhang, and X. Chen. 2019. DHAV-1 inhibits type I interferon signaling to assist viral adaption by increasing the expression of SOCS3. Front. Immunol. 10:731.

Xiaoyao, Y., Z. Qiurui, W. Mingshu, C. Anchun, P. Kangcheng, Z. Dekang, L. Mafeng, J. Renyong, Y. Qiao, W. Ying, C. Shun, Z. Xinxin, Z. Shaqiu, L. Yunya, Y. Yanling, and Z. Lin. 2018. DHAV-1 2A1 peptide - a newly discovered co-expression tool that mediates the ribosomal "skipping" function. Front. Microbiol. 9:2727.

Xie, Z., and D. J. Klionsky. 2007. Autophagosome formation: core machinery and adaptations. Nat. Cell Biol. 9:1102–1109.

Yang, M., A. C. Cheng, M. S. Wang, and H. Y. Xing. 2008. Development and application of a one-step real-time Taqman RT-PCR assay for detection of Duck hepatitis virus type1. J. Virol. Methods 153:55–60.

Yang, X., A. Cheng, M. Wang, R. Jia, K. Sun, K. Pan, Q. Yang, Y. Wu, D. Zhu, S. Chen, M. Liu, X. X. Zhao, and X. Chen. 2017. Structures and corresponding functions of five types of Picornaviral 2A. Proteins Front. Microbiol. 8:1373.

Zhang, J. K., Y. S. Li, C. D. Zhang, and D. Q. Dai. 2017. Up-regulation of CRKL by microRNA-335 methylation is associated with poor prognosis in gastric cancer. Cancer Cell Int. 17:28.

Zhou, S., S. Zhang, M. Wang, A. Cheng, D. Zhu, S. Chen, M. Liu, X. Zhao, R. Jia, Q. Yang, Y. Wu, S. Zhang, Y. Liu, Y. Yu, L. Zhang, and X. Chen. 2019. Development and evaluation of an indirect ELISA based on recombinant nonstructural protein 3A to detect antibodies to duck hepatitis A virus type 1. J. Virol. Methods 268:56–61.